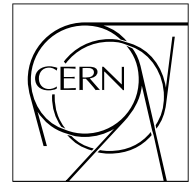


The Compact Muon Solenoid Experiment

CMS Note

Mailing address: CMS CERN, CH-1211 GENEVA 23, Switzerland



30 July 1998

A Review of the Magnetic Forces in the CMS Magnet Yoke

F. Kircher, V. Klioukhine^{*)}, B. Levesy

CEA/Saclay, Gif-sur-Yvette, France

S. Vorojtsov

JINR, Dubna, Russia

B. Curé, A. Desirelli, A. Hervé, H. Gerwig, J.P. Grillet

CERN, Geneva, Switzerland

R. Smith

FNAL, Batavia, IL, USA

Abstract

A summary of the magnetic forces, acting on various ferromagnetic parts of the flux-return yoke of the CMS magnetic system is presented. The latest information about the parameters of the system has been taken into account: coil revision 5/98, yoke revision 6/98, hadronic forward calorimeter revision 6/98. The Vector Fields TOSCA code and the modified CERN POISCR code were used for two- and three-dimensional finite-element calculations of the magnetic field. The forces on ferromagnetic elements were computed using the Maxwell surface integral method. The obtained results are compared with the estimates of the magnetic forces presented in the Magnet Technical Design Report.

^{*)} Visitor from Institute for High Energy Physics, Protvino, Russia

1 Problem formulation

The purpose of this work is to contribute to the new summary on magnetic forces, acting on various parts of the CMS magnetic system. The latest information about the parameters of the system has been taken into account: Coil revision 5/98 (Ref. [1]), Yoke revision 6/98, Hadronic Forward (HF) calorimeter revision 6/98.

The note compares the estimates of the magnetic forces made for the Magnet Technical Design Report (TDR) with recent two- and three-dimensional finite-element calculations, and with simpler engineering calculations. The results can be supplied to stress and deflection analyses so that judgments about the overall design conservatism of the barrel and end cap yokes can be made. The same analyses can predict the overall motion of the detector elements attached to the yokes so that required clearances between them can be maintained, especially in the case of the Hadronic End-cap (HE) calorimeter.

One of the issues of this calculations is to clarify the situation with the last disk of the HE-1 and the (ME-1)-(HE-1) interface system support tube (ST). These units were proposed to be manufactured from carbon steel instead of stainless steel. The obvious advantage of such a replacement is substantially lower cost of these structural units. The major concern is the B-field distortions and the magnetic forces that would act to the HE parts due to these pieces of iron.

2 Input Data and Methods

2.1 Magnetic system description

One eighth of the CMS magnetic flux return yoke considered for the computations is shown in Figs. 1 and 2. To calculate the forces on the last HE-1 disk a model with same symmetry is used as well.

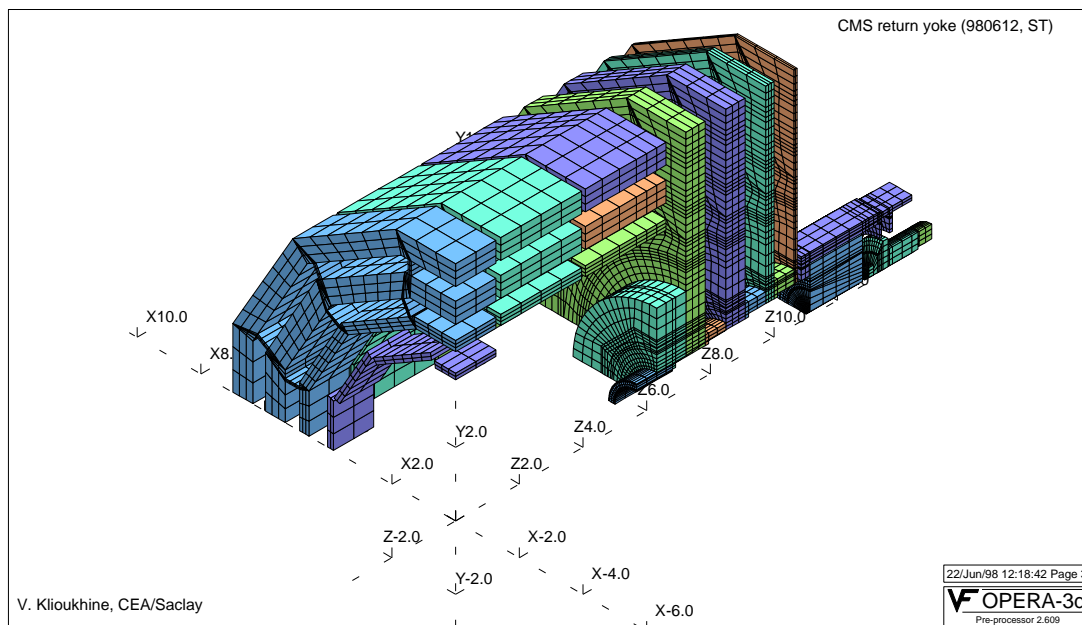


Figure 1: TOSCA computer model of the iron yoke of the magnetic system

The denotations of the system parts are given in Fig. 3, where the system layout is shown schematically and not to scale.

To describe the model we use the Cartesian coordinate system with an origin placed in the centre of the CMS solenoid. The direction of Z-axis is along the solenoid axis. The direction of Y-axis is upward.

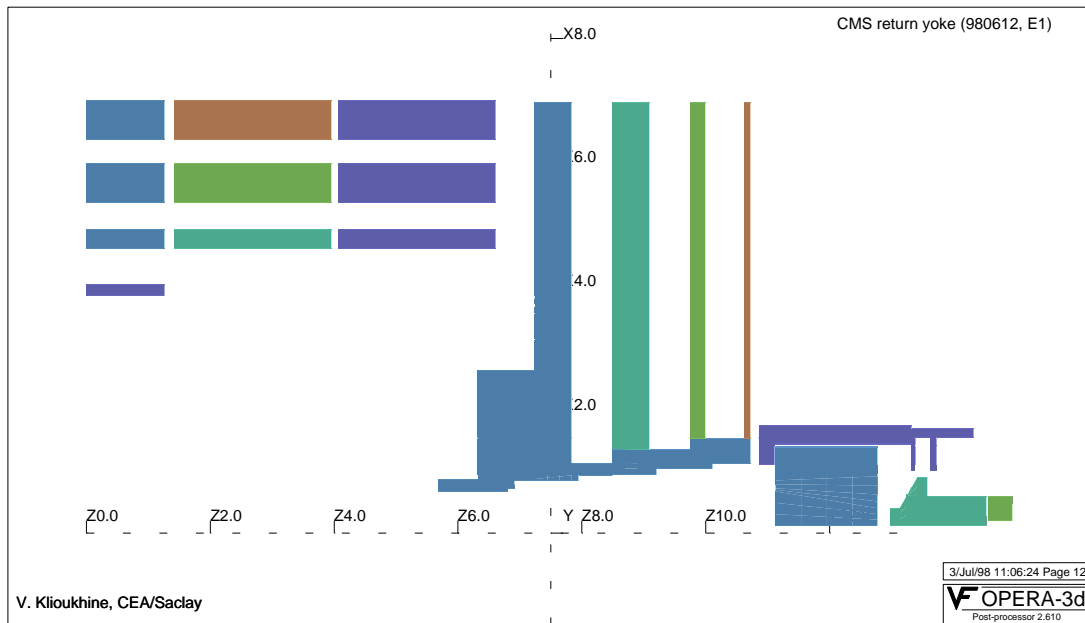


Figure 2: TOSCA computer model of the iron yoke of the magnetic system

The description of the model is as follows:

- The model of the solenoidal coil consists of five concentric but axially separated units. The units have lengths 6.16853, 3×0.00234 , and 6.16853 m and they are spaced axially from one another by 0.02021 m. Each unit consists of four coaxial layers of current each of radial thickness 0.0207 m at radii 3.17472, 3.23949, 3.30426, and 3.36903 m. The locations of the current layers correspond to the positions of the superconducting cable in the conductor when the coil is at cryogenic temperature. The overall axial length of the assembly is 12.42492 m. Three central units represent twelve central turns of the coil with a current in each turn of 19.5 kA. Two external units represent all the other turns of the coil and the current densities used in these units are 41.38585 MA/m². Thus, a total current in the coil is 42.51 MA-turns that gives 4.077 T in the centre of solenoid. The separation of twelve central turns is done to calculate the maximum magnetic flux densities near superconducting cable in each layer of coil. The calculated values are presented in Ref. [1].
- The CMS flux-return yoke consists of three 12-sided regular polygon-shaped assemblies: a barrel and two end-caps. The overall axial length of the barrel is 13.22 m and it is segmented axially into five sub-assemblies each of length 2.536 m with air gaps between of 0.12, 2×0.15 , and 0.12 m. Each barrel sub-assembly consists of three radial layers of steel of radial thickness 0.295 and 2×0.62 m thick. The inner layer of steel has an inscribed radius 4.61 m. There is an additional layer of steel 0.18 m thick in the Tail Catcher (TC), at an inscribed radius of 3.84 m, inside the central barrel sub-assembly. The brackets which space the iron layers in the sub-assemblies are included in the model.
- The full geometry of the barrel, end-caps and HF calorimeter is described in Tab. 1. The positions of the TC plates corners in XY -plane are shown in Tab. 2, the positions of brackets corners in the same plane are displayed in Tab. 3.

2.2 Magnetic properties of steel

The magnetic core is to be produced by Izhorsky Zavod of St. Petersburg. The B-H curve of the Izhora steel measured at CERN is selected as the most suitable one for the field simulations. The curve is close to that of GOST-08, but not quite the same.

The steel has been measured up to 1.9571 T. For higher fields we use for the time being the GOST-08 curve, which is reported here as well. The combined curve used in the B-field simulation codes is shown in Figs. 4 and 5.

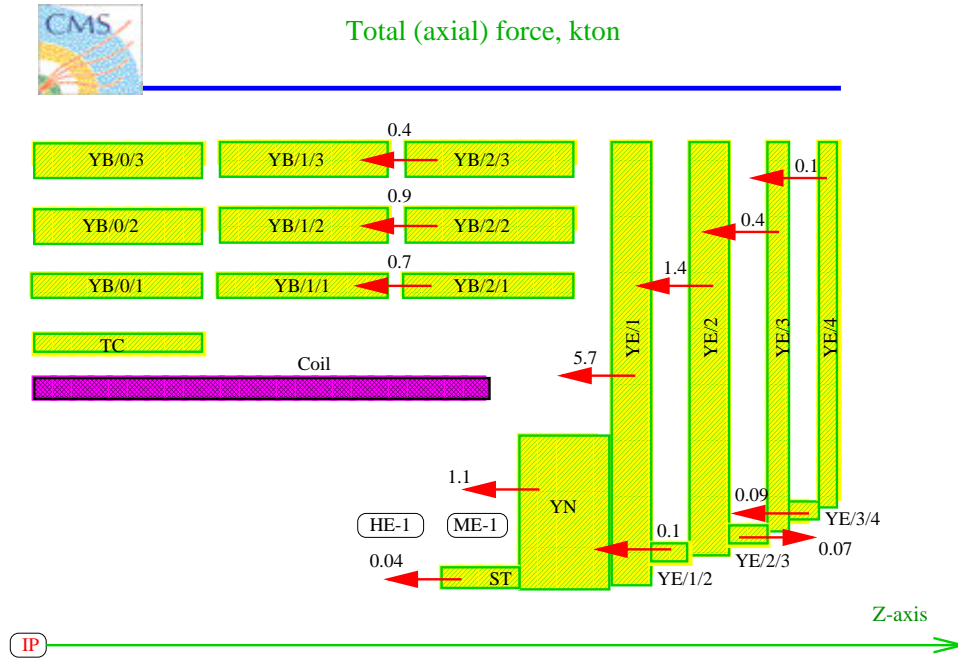


Figure 3: Volume force distribution (Surf. int.)

The corresponding magnetization saturation level, which is characteristic of the given type of steel, is equal to 2.135 T according to these data.

3 Computer codes and methods

The Vector Fields TOSCA code, version 6.6 (Ref. [2]) and the modified CERN POISCR code (Ref. [3]) are used for the field analysis of the magnetic field distribution in the CMS magnetic system. The TOSCA computer model is generated according to the approach, given in Refs. [4, 5].

The OPERA-3D (Ref. [6]) is used to integrate the Maxwell Stress tensor over the surfaces of the yoke pieces for obtaining the forces on the iron. These forces are presented in Tab. 4 under the column heading TOSCA Surf. int. The integration surfaces pass through ferromagnetic material. Thus, an infinitely thin gap at the integration surface is assumed and the following formula is used:

$$\mathbf{F} = \int_S [\mathbf{H}_a (\mathbf{B} \cdot \mathbf{n}) - \frac{\mu_0}{2} (\mathbf{H}_a \cdot \mathbf{H}_a) \mathbf{n}] dS, \quad (1)$$

where

$$\mathbf{H}_a = \mathbf{H} + \left(\frac{1}{\mu_0} \mathbf{B} - \mathbf{H} \right) \cdot \mathbf{n} \mathbf{n},$$

\mathbf{B} is a vector of the magnetic flux density,

\mathbf{H} is a vector of the magnetic field strength,

\mathbf{n} is a normal unit vector external to surface of region,

$$\mu_0 = 4\pi \cdot 10^{-7} \frac{V \cdot s}{A \cdot m}.$$

To get a feeling of the order of magnitude of the forces, some engineering estimation, based on the reduced version of the previous formula, is also used (Eng. est.). In this estimation, used the values of the magnetic flux density calculated with the TOSCA model, it is assumed that on a material surface the normal field component value from the air-side of the interface gives a major contribution to the force, thus, an axial force can be expressed as $\frac{B_z^2}{2\mu_0}$, where B_z is an axial component of the magnetic flux density. The force is always directed along the outside normal unit vector to the iron surface. In contrary to the method, given above, only the iron-air interface considered here. The perfect azimuthal symmetry of the field map is also implied. This method showed good results (see for example Ref. [7]) and as it can be seen below is quite justified in our case.

Table 1: Geometry of the flux-return yoke.

Unit	Inner radius, m	Outer radius, m	$ z_{min} , m$	$ z_{max} , m$
YB/0/1	4.610*	4.905*	-1.268	1.268
YB/0/2	5.350*	5.970*	-1.268	1.268
YB/0/3	6.375*	6.995*	-1.268	1.268
YB/1/1	4.610*	4.905*	1.418	3.954
YB/1/2	5.350*	5.970*	1.418	3.954
YB/1/3	6.375*	6.995*	1.418	3.954
YB/2/1	4.610*	4.905*	4.074	6.610
YB/2/2	5.350*	5.970*	4.074	6.610
YB/2/3	6.375*	6.995*	4.074	6.610
TC	3.840*	4.020*	-1.268	1.268
ST	0.675	0.875	5.680	6.320
”	0.675	0.850	6.320	6.810
YN/1	0.850	2.630	6.320	6.810
YN/2	0.725	2.630	6.810	6.910
”	0.850	2.630	6.910	7.240
YE/1	0.850	6.955*	7.240	7.840
YE/1/2	0.850	1.135	7.840	7.950
”	0.935	1.135	7.950	8.495
YE/2	0.950	6.955*	8.495	9.095
YE/2/3	0.950	1.360	9.095	9.205
”	1.040	1.360	9.205	9.750
YE/3	1.040	6.955*	9.750	10.000
YE/3/4	1.040	1.530	10.000	10.110
”	1.130	1.530	10.110	10.630
YE/4	1.130	6.955*	10.630	10.730
HF/0	0.125	1.400	11.130	12.780
HF/1	1.108	1.750*	10.860	11.110
”	1.450*	1.750*	11.110	13.330
”	1.550*	1.700*	13.330	14.330
”	1.020	1.550*	13.330	13.380
”	1.020	1.550*	13.630	13.730
HF/2	0.130	0.400	12.980	13.130
”	0.130	0.900	13.4187	13.580
”	0.130	0.600	13.580	14.530
HF/3	0.200	0.600	14.560	14.960

* Inscribed radius

Table 2: Positions of TC plates corners.

Azimuth, deg.	0–20	20–50	50–80	80–90
x_1, m	3.84000	3.64442	2.47232	0.63776
y_1, m	0.00000	1.36768	3.00666	3.84000
x_2, m	3.84000	2.65555	0.75954	0.00000
y_2, m	1.33998	3.08046	3.99553	3.84000
x_3, m	4.02000	2.77868	0.79281	0.00000
y_3, m	1.40549	3.22719	4.18417	4.02000
x_4, m	4.02000	3.81617	2.58980	0.66950
y_4, m	0.00000	1.43020	3.14667	4.02000

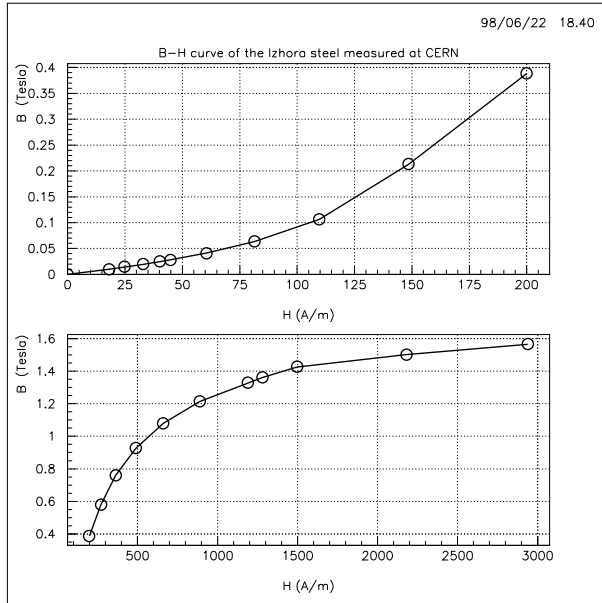


Figure 4: B-H curve used in the calculations

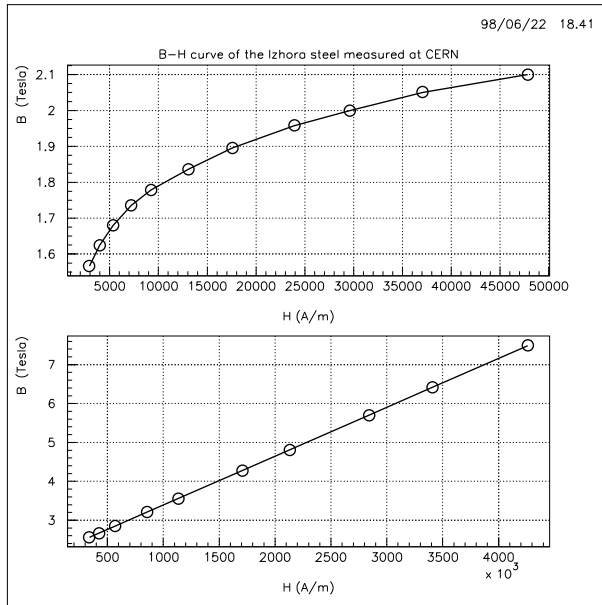


Figure 5: B-H curve used in the calculations

Table 3: Positions of brackets corners.

Azimuth, deg.	0–15	15–30	30–45	45–60	60–75	75–90
x_1, m	4.90500	5.86699	3.64752	4.19193	1.41268	1.39364
y_1, m	1.20068	1.77807	3.49232	4.47335	4.84819	5.97000
x_2, m	5.35000	6.21773	4.03290	4.39443	1.63518	1.39364
y_2, m	1.20068	1.98057	3.71482	4.82409	5.23358	6.37500
x_3, m	5.35000	6.26773	4.07040	4.48103	1.70013	1.49364
y_3, m	1.12568	1.89397	3.64987	4.77409	5.19608	6.37500
x_4, m	4.90500	5.91699	3.68502	4.27853	1.47763	1.49364
y_4, m	1.12568	1.69147	3.42737	4.42335	4.81069	5.97000

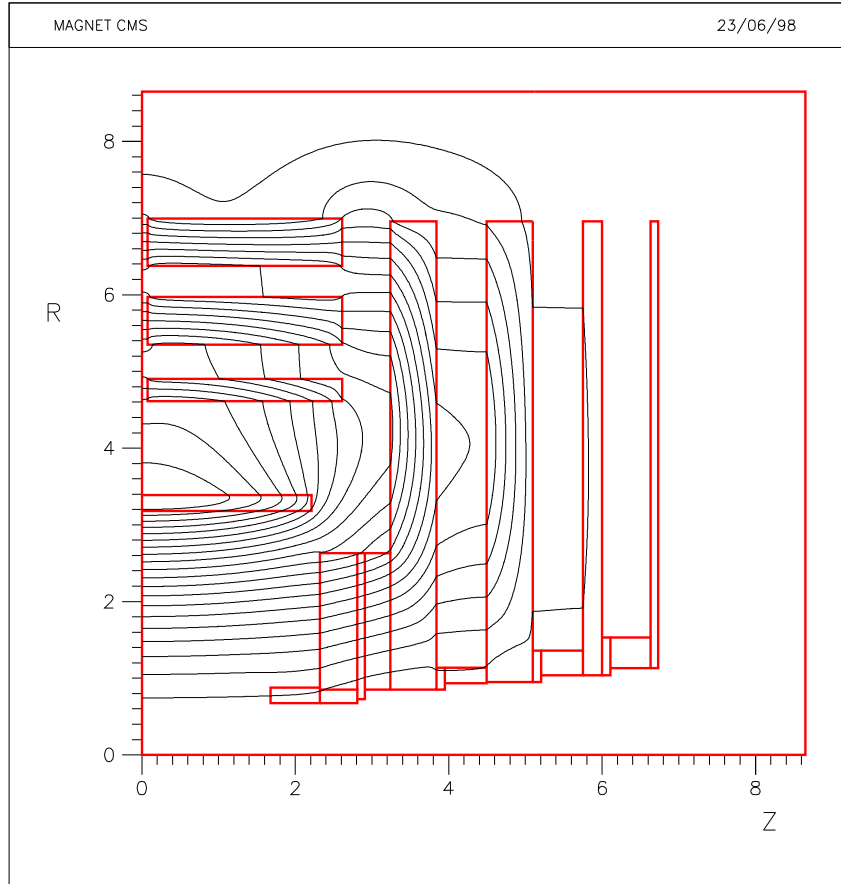


Figure 6: POISCR 2d computer model of the magnet

To cross-check the TOSCA results, the simplified POISCR 2d computer model, shown in Fig. 6, is used. Only the end-cap region is included into the model to facilitate the best description of the magnet structure within the limited number of the grid nodes.

4 Previous calculations

The previous results on the magnetic force calculations are presented in Ref. [8] (see Fig. 7 and the second (TDR) column of Tab. 4).

The total force, acting on the selected structure unit, is an axial force with the corresponding sign showing the direction of the force. The reason for this is the fact that the total radial force, acting on the unit, is zero due to the symmetry of the system geometry. The negative sign of the force means the force directed to the Interaction Point (IP), inwards the detector.

Table 4: Total forces (kton).

Case	TDR	TOSCA		POISCR	TOSCA	
Variant	No ST	ST	No ST	ST		
Method	-	Surf. int.			Eng. est.	
Force at	Iron volume			Iron-air interface		
Unit						
YB/0/1	-0.68	-	-	-	-	-
YB/0/2	-1.26	-	-	-	-	-
YB/0/3	-1.61	-	-	-	-	-
YB/1/1	-	-	-	-	+0.10	+0.06
YB/1/2	-	-	-	-	-0.05	-0.08
YB/1/3	-	-	-	-	-0.22	-0.18
YB/1/1+2+3	-	-0.17	-0.18	-	-0.17	-0.20
YB/2/1	-	-0.36	-0.40	-0.7	-0.36	-0.32
YB/2/2	-	-0.88	-0.88	-1.4	-0.88	-0.78
YB/2/3	-	-0.75	-0.75	-1.1	-0.75	-0.68
YE/1	-4.91	-5.73	-5.69	-5.9	-	-
YE/2	-1.70	-1.36	-1.32	-1.8	-1.15	-1.22
YE/3	-0.15	-0.37	-0.38	-0.4	-0.005	-0.01
YE/4	-	-0.09	-0.09	+0.1	+0.00	-
YN	-2.01	-1.10	-1.11	-1.5	-	-
YE/1+YN+ST	-6.93	-6.87	-	-7.56	-5.98	-6.59
YE/1/2	-	-0.11	-0.10	-0.01	-	-
YE/2/3	-	+0.07	+0.07	+0.07	-	-
YE/3/4	-	-0.09	-0.08	-0.07	-	-
TC	-	-	-	-	-	-
ST	-	-0.04	-	-0.16	-	-
HF/0	-	-0.00	-0.00	-	-0.00	-
HF/1	-	-0.00	-0.00	-	-0.00	-
HF/2	-	+0.00	+0.00	-	+0.00	-
HF/3	-	-0.00	-0.00	-	-0.00	-

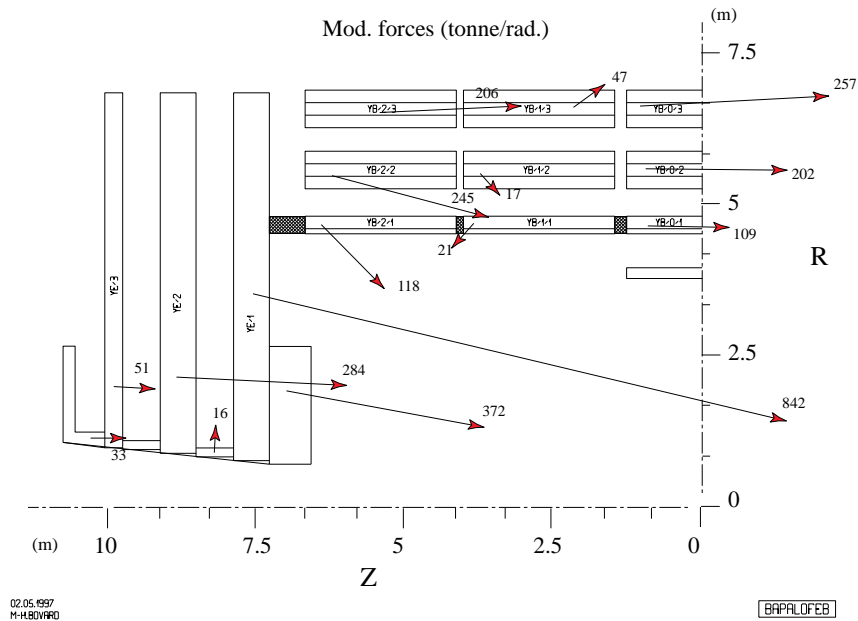


Figure 7: TDR magnetic force distribution

5 Results

In the third and fourth columns of Tab. 4 the axial force values obtained with TOSCA code using Eq. 1 are shown. These values are displayed in Fig. 3 for the case of ST installed. The forces are obtained by the integration over surfaces of the yoke pieces exactly described in Tab. 1–3. The sixth column of Tab. 4 contains the values of axial forces obtained by the integration over surfaces marked in Fig. 2 by different colors. In such a case the integration surfaces do not pass through the iron in the regions where the magnetic flux density vector is orthogonal to the integration surface. That means that the surfaces of integration are mostly the iron-air interface surfaces.

The forces applied to various iron-air interface surfaces using Eng. est. are given in Fig. 8 and Fig. 9 (the ST installed) and are shown in the last column of Tab. 4.

In all these Figures the only forces starting from a certain level of magnitude are displayed. For some units (except the coil) the forces are below this level and are not shown in the Figures for clarity.

Comparison of the force magnitudes obtained using Eq. 1 with the corresponding TDR results shows that they more or less agree. There are still several disagreements between the TDR and given calculations. The YN-force is about twice smaller (but the total force, acting on YN+YE/1 is about the same in all cases) and the YE/3-force is about twice larger in the given calculations. Radial force components at the YN and YE/1 in Eng. est. have directions opposite to that ones from the TDR results. These disagreements could probably be explained by the differences in the geometry and B-H curves in two calculations.

The variants with and without the hadronic end-cap calorimeter support tube are practically identical as far as the force distributions concerned. Basically, the ST contribution is in that sense an effect of the second order.

Comparison of the TOSCA results based on the iron-air interface surface integration with the engineering estimation shows in general reasonably good agreement ($\approx 10\%$) between both methods (see the last two columns of Tab. 4).

The direct application of the POISCR routine FORCCR gives the results, shown in the fifth column of Tab. 4. There is some agreement of the TOSCA and POISCR solutions for practically all of the units. The flux line map in Fig. 6 gives a good explanation of the sign of the calculated forces: iron-parts are always pulled in the direction of the region with the larger absolute value of field.

Using the POISCR produced field map in the vicinity of the iron-air interface and applying the (Eng. est.) method it is possible to additionally cross-check forces for some of the units. The results in general confirm the TOSCA calculations. For example, for the ST surface at $Z=5.68$ m the total (axial) force is calculated from the POISCR data at the level of -0.55 kton, which could be compared with the TOSCA+(Eng. est.) value of -0.42 kton with the $\approx 30\%$ difference between two results.



Axial iron-air interface force (kton)

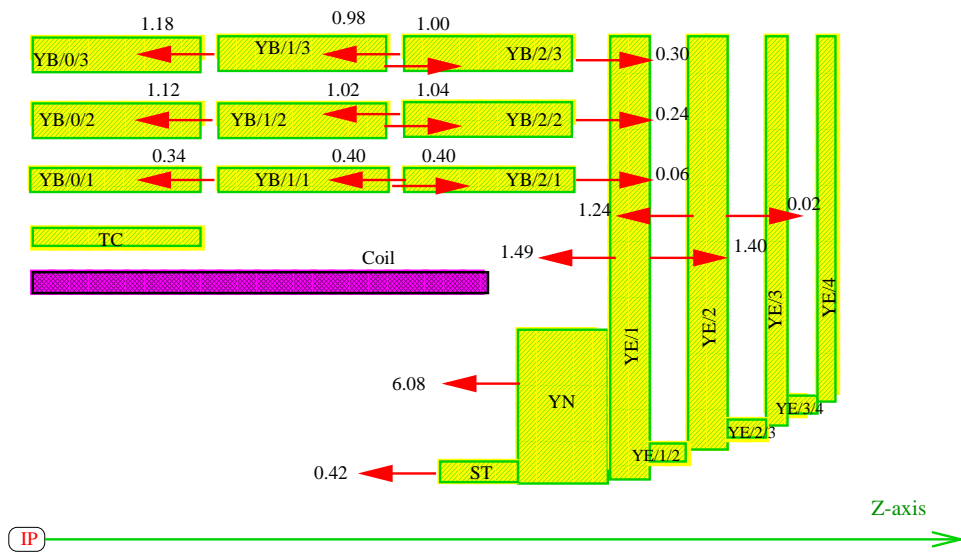


Figure 8: Axial surface force distribution (Eng. est.)



Radial iron-air interface force (kton/radian)

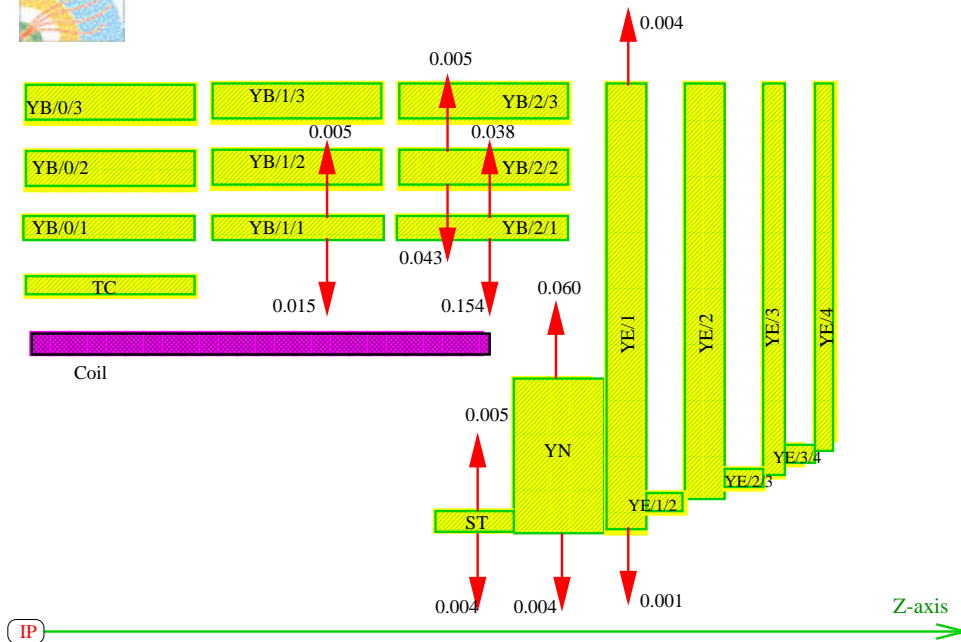


Figure 9: Radial surface force distribution (Eng. est.)

One also could try the VF OPERA-2d application for this case to increase the reliability of the results presented here.

Concerning an estimation of force, acting on the last disk of the HE-1, it shows the positive total force value of 0.2 kton in the case when this unit is manufactured from carbon steel instead of stainless steel. This disk produces also severe distortion (large gradient of the B_r component) in the ME-1 region. So, it is recommended to replace this disk to a non-magnetic one.

6 Conclusions

- The present force estimate confirms in general the calculations given in Ref. [8].
- There are still several disagreements between the TDR and given calculations. These disagreements could probably be explained by the differences in the geometry and B-H curves in two calculations.
- Obtained detailed distribution of forces along the border of various parts of the system is valuable to understand the mechanics of system performance.

7 Future Plans

There are several issues still to be covered by the future computations:

- Magnetic forces acting on coil. Distribution of these forces.
- Various forces which appear due to the geometry misalignments of system parts. In particular, the forces on the iron pieces caused by the coil axial misalignment. One should check if this will effect the central parts of the barrel yoke.
- Force variation due to displacement of the geometrical position of the system units when the coil current is on. The specific values of these displacements depend on the adopted design of the system and are not completely certain presently.
- Force linear density distributions. Torques.

References

- [1] **DSM/DAPNIA/STCM Technical Report 5C 2100T-0000 057 PB, 14 May 1998**, B. Levesy, "*CMS COIL PARAMETER BOOK*".
- [2] Vector Fields Limited, 24 Bankside, Kidlington, Oxford OX5 1JE, England.
- [3] **CERN Computer Newsletter 217 (1994) 18-19**, V.I. Klyukhin, B.I. Klochkov, "*A Second Life of the CERN POISSON Program Package*".
- [4] **DSM/DAPNIA/STCM Technical Report 5C 2100T-M 1000 020 97, 8 July 1997**, V. Klioukhine, "*Calculation of Magnetic Forces on the CMS Coil with TOSCA*".
- [5] **DSM/DAPNIA/STCM Technical Report 5C 2100T-M 1000 023 97, 22 August 1997**. V. Klioukhine, "*Magnetic Forces in the CMS Magnetic System Calculated with TOSCA*".
- [6] **VF-01-98-D4**, Vector Fields Limited, 24 Bankside, Kidlington, Oxford OX5 1JE, England, "*OPERA-3d Reference Manual*".
- [7] **ATL-TILECAL-98-137 (ATL-L-PN-137), 27 January 1998**, S. Vorojtsov et al., "*Calculation of the TileCal Magnetic Forces using 3D TOSCA Model*".
- [8] **CERN/LHCC 97-10, CMS TDR 1, 2 May 1997**, "*CMS. The Magnet Project. Technical Design Report*".